

On the optical response of 2D systems: Insights of classical electromagnetism to *ab initio* calculation

Stefano Mazzei* and Christine Giorgetti†
LSI, CNRS, Ecole Polytechnique, CEA/DRF/IRAMIS,
Institut Polytechnique de Paris, F-91128 Palaiseau

and European Theoretical Spectroscopy Facility, 91128 Palaiseau, France

(Dated: August 1, 2022)

ABSTRACT

Quasi-2D objects appear to be promising for the development of new optical devices, since their electronic properties are expected to be governed by their size. The understanding of these properties can be achieved by means of theoretical spectroscopy based on the state-of-the-art *ab initio* formalisms. Time-dependent density functional theory is well suited since it accounts for the local field effects, which are expected to be large at the interfaces with vacuum. This framework allows the calculation of the response function to the external potential. For bulk materials, this quantity is related to the macroscopic dielectric function following the Adler and Wiser formula. This expression contains dimensionless quantities, while for 2D object, the physical observables should be proportional to the thickness. In this paper, we propose a mixed-space approach which allows us to calculate in a direct way the out-of-plane component and to evidence how the ambiguity on the thickness of the slab affects the calculation of the macroscopic dielectric function. The classical Lorentz model adapted to a thin slab reveals how the huge change of the induced electric field, and the arising of a transverse polarization, lead to modify the expression of the macroscopic dielectric function to get the absorption spectrum. Despite the influence of the thickness of the slab on the macroscopic dielectric function, the optical response resulting from the classical electromagnetism can be unambiguously calculated from the mixed-space simulations.

I. INTRODUCTION

Objects of reduced dimensionality are promising building blocks for new technological devices [1, 2]. At the nanometric scale, the electronic properties, and thus the response to an excitation, are expected to exhibit different features from the bulk counterpart, due to the electronic confinement: screening effects should be reduced and the band gap should be modified [3–6]. Development of these new devices relies on the understanding of their electronic properties. Theoretical spectroscopy based on *ab initio* formalism is state of the art [7]. Time-dependent density functional theory (TD-DFT) [8–11] is a tool of choice which allows one in principle to account for the many-body effects [12], by solving the so-called Dyson equation. Very efficient numerical codes have been developed in the reciprocal space to take benefit from the periodicity of infinite crystals. The quantity resulting from the Dyson equation is the microscopic density response function $\chi_{\mathbf{G}\mathbf{G}'}(\mathbf{q};\omega)$, expressed as a matrix on the basis of the reciprocal space vectors \mathbf{G} . It allows to calculate the inverse dielectric matrix:

$$\varepsilon_{\mathbf{G}\mathbf{G}'}^{-1} = \delta_{\mathbf{G}\mathbf{G}'} + v_{\mathbf{G}}(\mathbf{q}) \chi_{\mathbf{G}\mathbf{G}'}(\mathbf{q};\omega) \quad (1)$$

where $v_{\mathbf{G}}(\mathbf{q}) = 4\pi/|\mathbf{G} + \mathbf{q}|^2$ is the Coulomb potential. The absorption spectrum is the imaginary part of the

macroscopic dielectric function $\varepsilon_M(\mathbf{q} \rightarrow 0; \omega)$ given by the Adler and Wiser formula [13–15]

$$\varepsilon_M^{LL}(\mathbf{q} \rightarrow 0; \omega) = \frac{1}{\varepsilon_{00}^{-1}(\mathbf{q} \rightarrow 0; \omega)} \quad (2)$$

When one considers isolated nano-objects, which are finite in one or several directions, one uses the supercell approach, where the object is embedded in vacuum. Many difficulties arise. The bare Coulomb interaction cannot be used anymore, since it would reproduce the unphysical interaction between replicas, and it must be replaced with a truncated interaction [16, 17]. One must also be careful to avoid spurious effects coming from the presence of vacuum in the supercell [18]. Since the discovery of graphene [19], the case of 2D and quasi-2D crystal attracted a huge interest. Using a truncated Coulombian interaction [16, 17], Hüser and coworkers [20] calculated the potential induced by an isolated MoS₂ monolayer, and obtained the static dielectric function of the 2D system as:

$$\varepsilon_M^{2D}(\mathbf{q}) = \frac{\langle V^{ext}(\mathbf{q}) \rangle_d}{\langle V^{tot}(\mathbf{q}) \rangle_d} \quad (3)$$

(where $\langle \cdot \rangle_d$ stands for the average over a region of thickness d). They reported that, in the long-wavelength limit, $\varepsilon_M^{2D}(\mathbf{q} \rightarrow 0) \approx 1$, which reflects the reduction of the screening occurring in a very thin film. For this reason, such an approach has been successfully applied to model the screening in GW calculations on 2D materials [21, 22]. To make things even more puzzling, there is quite a wide agreement in literature that the quantity defined by Eq.

* stefanomazzei@gmail.com

† christine.giorgetti@polytechnique.edu;
<https://etsf.polytechnique.fr/People/Christine>

(3) should not be used to describe optical properties. The dielectric function extracted from ellipsometric measurements [23, 24] does not exhibit the behavior of the one calculated from Eq. (3), and as pointed out by several authors [25][26], the quantity which should be linked to the absorption is not the 2D-dielectric function but the 2D-polarisability α_{2D} (see e.g. Ref. [26]):

$$\varepsilon^{eff} = 1 + \frac{4\pi}{d}\alpha_{2D} \quad (4)$$

with d the thickness of the slab, and where:

$$\alpha_{2D} \propto -\frac{L_{SC}}{|\mathbf{q}|^2}\chi_{\mathbf{00}}(\mathbf{q}). \quad (5)$$

L_{SC} is the size of the supercell, \mathbf{q} an in-plane vanishing reciprocal space vector, and $\chi_{\mathbf{00}}$ has been calculated with the truncated Coulomb potential [16, 17]. The dielectric function defined in Eq. (4) is proportional to the macroscopic average of the χ response function, which is different from Eqs. (1) and (2). Moreover, when dealing with 2D objects, the notion of macroscopic average is not well defined. For strictly 2D objects, Cudazzo *et al.* [27] proposed to calculate

$$\varepsilon = 1 + 2\pi|\mathbf{q}|\alpha_{2D}$$

where \mathbf{q} is an in-plane reciprocal space vector, and α_{2D} can be calculated from a 3D (i.e. without truncated Coulomb interaction) TD-DFT calculation in a supercell according to

$$\alpha_{2D} = L_{SC} \frac{\varepsilon_M^{3D} - 1}{4\pi} = \frac{L_{SC}}{4\pi} \left[\frac{1}{1 + \lim_{\mathbf{q} \rightarrow 0} \frac{4\pi}{|\mathbf{q}|^2} \chi_{\mathbf{00}}(\mathbf{q})} - 1 \right] \quad (6)$$

For a quasi-2D object, the physical quantities are expected to be proportional to the thickness of the object. The dimension of a length is recovered due to L_{SC} in the expression of α_{2D} (Eq. (5) or (6)). But this factor is not the thickness of the object, which also reveals delicate to define. It is usually taken as a ratio of the bulk unit cell. Nevertheless, it should act as a scaling factor, with the spectral shape given by $\chi_{\mathbf{00}}$ (for Eq. (5)) or ε_M^{3D} (for Eq. (6)). But due to the supercell formalism, the question of the normalization of χ arises, in particular when it enters in Eqs. (2) or Eq. (6). Finally, these formalisms concern the in-plane excitation. To calculate the out-of-plane component, the expression

$$\varepsilon_{2D,\perp} = \left[1 + \frac{L_{SC}}{d} \left(\frac{1}{\varepsilon_{SC,\perp}} - 1 \right) \right]^{-1} \quad (7)$$

has been proposed [28], which results from the fact that the quantity calculated within the supercell SC framework is an effective medium theory (EMT) [29] between the 2D object and the vacuum [18], and where the value of d has a strong influence. As we can see from these different approaches, the question of the definition of

the dielectric function of the 2D object, its relation with the screening, and the subtle point of the normalization procedure, requires further clarification. We highlight that the problem is not related to the distinction between the 2D-dielectric function or the 2D-polarisability [26, 27, 30, 31]. Indeed, the 2D-polarisability is independent of the size of the supercell due to a renormalization with this factor. In the case of the in-plane component, $\alpha_{2D}^{\parallel} \propto L_{SC}(\varepsilon_{SC}^{\parallel} - 1)$, so α_{2D}^{\parallel} and $\varepsilon_{SC}^{\parallel}$ exhibit the same spectral features. For the out-of-plane component, $\alpha_{2D}^{\perp} \propto L_{SC}(1 - 1/\varepsilon_{SC}^{\perp})$, where $1/\varepsilon_{SC}^{\perp}$ corresponds to the definition of the plasmon, and cannot account for the absorption process of a photon. For these reasons, and to allow the comparison with the bulk counterpart, we will still focus on the calculation of the dielectric function.

In this paper, using the Lorentz model, we evidenced the electronic properties of 2D objects, which allows the demonstration of the expression of the macroscopic dielectric function, in order to calculate the absorption spectrum. For the in-plane component, we show that it cannot be calculated from the ratio of the macroscopic average of the external and total electric potentials, like for 3D systems. For the out-of-plane component, the use of the Adler and Wiser formula should in principle be valid to calculate the absorption spectrum from the *ab initio* TD-DFT framework. Nevertheless, we also show, by the mean of a mixed-space approach, that the dependence of the spectrum extracted from this formula with the normalization procedure, goes much beyond the problem of the vacuum introduced in the supercell but leads to the question of the thickness of the matter of the 2D object, which reveals ambiguously defined. We finally show that this ambiguity has no consequence on the measured optical quantities like absorbance or transmittance.

As a prototypical system, we use a slab of silicon cut in the (001) direction, with a surface reconstruction (2×1) [32], composed of four conventional cubic cells leading to an atomic thickness of $4 \times 10.263 = 41.052$ bohrs before relaxation and ~ 40 bohrs after. The y direction is perpendicular to the dimers and z is orthogonal to the surface. This system is not, *stricto sensu*, a 2D material, since the binding in the z direction is as large as in-plane. However, in a technical perspective, the treatment is equivalent. Moreover, it presents the advantage to have the absorption and plasmon resonances very far in energy.

The paper is organized as following: In Sec. (II), alternatively to the usual procedure, we proposed a mixed-space approach to calculate directly the out-of-plane component within TD-DFT. It shows how the Adler and Wiser formula suffers from the definition of the thickness of the slab. To understand the feature of these *ab initio* results, we adapted in Sec. (III) the classical Lorentz model to the case of a finite slab, which explains how the huge change of the induced electric field modifies the calculation of the macroscopic dielectric function giving the absorption spectrum for the in-plane component. De-

spite the influence of the definition of the thickness of the slab on the optical response, we show in Sec. (IV) that the reflectance and transmittance of a thin slab resulting from classical electromagnetism can be unambiguously calculated from the mixed-space simulations.

II. TD-DFT: MIXED-SPACE APPROACH

A. Dyson equation

In this approach, the in-plane directions - where the system is infinite and periodic - are treated in the reciprocal space, while the out-of-plane direction (taken along z) - where the system is finite and the periodicity broken - is treated in the real space. The starting point of our calculation is the Kohn-Sham structure evaluated within DFT-LDA [33, 34] using ABINIT [35], followed

by the independent particle response function, obtained in reciprocal space via DP-CODE [36]. Its mixed-space representation is obtained as:

$$\begin{aligned} \chi_{\mathbf{G}\mathbf{G}'}^0(\mathbf{q}, \omega) &\longrightarrow \chi_{\mathbf{G}_{\parallel}\mathbf{G}'_{\parallel}}^0(\mathbf{q}_{\parallel}, z, z', \omega) \\ &= \frac{1}{L_z} \sum_{G_z, G'_z} e^{-i(G_z+q_z)z} \chi_{\mathbf{G}\mathbf{G}'}^0(\mathbf{q}, \omega) e^{i(q_z+G'_z)z'} \end{aligned}$$

Since we are interested in the definition of interfaces, characterised by a huge change of the electronic density, we will work in the random phase approximation (RPA), which neglects the exchange and correlation effects, but accounts for the response of the matter at the atomic scale, the so-called local field effects (LFE), through the Hartree potential v^{coul} . The Dyson equation in the mixed-space reads as

$$\begin{aligned} \chi_{\mathbf{G}_{\parallel}\mathbf{G}'_{\parallel}}(\mathbf{q}_{\parallel}, z, z', \omega) &= \chi_{\mathbf{G}_{\parallel}\mathbf{G}'_{\parallel}}^0(\mathbf{q}_{\parallel}, z, z', \omega) + \\ &+ \sum_{\mathbf{G}_{1\parallel}\mathbf{G}_{2\parallel}} \int_{-\infty}^{\infty} dz_1 \int_{-\infty}^{\infty} dz_2 \chi_{\mathbf{G}_{1\parallel}\mathbf{G}_{1\parallel}}^0(\mathbf{q}_{\parallel}, z, z_1, \omega) v_{\mathbf{G}_{1\parallel}\mathbf{G}_{2\parallel}}^{coul}(\mathbf{q}_{\parallel}, z_1, z_2) \chi_{\mathbf{G}_{2\parallel}\mathbf{G}'_{\parallel}}(\mathbf{q}_{\parallel}, z_2, z', \omega) \end{aligned} \quad (8)$$

We stress out that Eq. (8) is equivalent to its reciprocal space representation and depicts a system infinite and periodic in all directions. Indeed, the integration in z_1 and z_2 is performed from $-\infty$ to $+\infty$, meaning that the Hartree potential felt by the electrons will be the potential induced by all the replicas. To get the response of the isolated slab, we have to eliminate the potential induced by the replicas. This can be achieved applying a cut-off

in the z direction to the Coulomb potential operator[16]:

$$\begin{aligned} v^{coul}(\mathbf{q}_{\parallel}, z, z') &\longrightarrow \tilde{v}^{coul}(\mathbf{q}_{\parallel}, z, z') \\ &= \Theta(z + \frac{L}{2})\Theta(-z + \frac{L}{2})v^{coul}(\mathbf{q}_{\parallel}, z, z')\Theta(z' + \frac{L}{2})\Theta(-z' + \frac{L}{2}) \end{aligned} \quad (9)$$

Substituting (9) in Eq. (8), we obtain the Dyson equation for an isolated slab:

$$\begin{aligned} \chi_{\mathbf{G}_{\parallel}\mathbf{G}'_{\parallel}}(\mathbf{q}_{\parallel}, z, z', \omega) &= \chi_{\mathbf{G}_{\parallel}\mathbf{G}'_{\parallel}}^0(\mathbf{q}_{\parallel}, z, z', \omega) + \\ &+ \sum_{\mathbf{G}_{1\parallel}\mathbf{G}_{2\parallel}} \int_{-L/2}^{L/2} dz_1 \int_{-L/2}^{L/2} dz_2 \chi_{\mathbf{G}_{1\parallel}\mathbf{G}_{1\parallel}}^0(\mathbf{q}_{\parallel}, z, z_1, \omega) v_{\mathbf{G}_{1\parallel}\mathbf{G}_{2\parallel}}^{coul}(\mathbf{q}_{\parallel}, z_1, z_2) \chi_{\mathbf{G}_{2\parallel}\mathbf{G}'_{\parallel}}(\mathbf{q}_{\parallel}, z_2, z', \omega) \end{aligned} \quad (10)$$

B. Mixed-space representation of the Coulomb potential operator

In the mixed-space representation, the Coulomb potential operator is:

$$v_{\mathbf{G}_{\parallel}\mathbf{G}'_{\parallel}}^{coul}(\mathbf{q}_{\parallel}, z, z') = \delta_{\mathbf{G}_{\parallel}\mathbf{G}'_{\parallel}} \frac{2\pi}{|\mathbf{q}_{\parallel} + \mathbf{G}_{\parallel}|} e^{-|\mathbf{q}_{\parallel} + \mathbf{G}_{\parallel}| |z-z'|} \quad (11)$$

It is the electrostatic potential induced by a planar charge distribution modulated in the in-plane direction by an

oscillation of wave vector $\mathbf{q}_{\parallel} + \mathbf{G}_{\parallel}$. This expression is divergent for $\mathbf{q}_{\parallel} + \mathbf{G}_{\parallel} = 0$. In Ref. 18, we solved the Dyson equation with this diverging potential, which requires to calculate ε_M for (q_{\parallel}) , $(q_{\parallel} + q_z)$ and $(q_{\parallel} - q_z)$ and to extract the q_z component from a linear combination. Moreover, the purpose of this previous work was to mimic a surface, namely a very thick slab, so the value of $|q|$ was set to ~ 1 [37], in order to fulfill the con-

dition $|q_{\parallel}|L/2 \gg 1$.¹ In the present work, we focus on the ultra-thin object in the optical limit, so we keep a vanishing \mathbf{q} vector. Moreover, we want to describe the response of the system to an external perturbation directed out of plane (i.e. having $\mathbf{q}_{\parallel} \equiv 0$). v^{coul} for $\mathbf{q}_{\parallel} + \mathbf{G}_{\parallel} = 0$ corresponds to the potential created by a planar and homogeneous distribution of charge. An infinite positively (negatively) homogeneously charged plane induces an electric field constant and uniform diverging from (converging to) the plane. The Coulomb potential operator in the mixed-space representation is thus given, for $\mathbf{q}_{\parallel} \equiv 0$, by:

$$v_{\mathbf{G}_{\parallel}\mathbf{G}'_{\parallel}}^{coul}(\mathbf{q}_{\parallel} = 0, z, z') = \delta_{\mathbf{G}_{\parallel}\mathbf{G}'_{\parallel}} \times \begin{cases} -2\pi|z - z'| & \text{for } \mathbf{G}_{\parallel} = 0 \\ \frac{2\pi}{|\mathbf{G}_{\parallel}|} e^{-|\mathbf{G}_{\parallel}||z-z'|} & \text{for } \mathbf{G}_{\parallel} \neq 0 \end{cases}$$

C. Out-of-plane response and the L_{mat} problem

The independent particle response function has been calculated in the optical limit ($\mathbf{q} = 10^{-5}$ bohrs⁻¹, with $\mathbf{q} = q\hat{\mathbf{z}}$). Since we expect the local fields to be weak in the in-plane direction [38], we evaluated the $\chi_{\mathbf{G}\mathbf{G}'}^0$ on a set of \mathbf{G} -vectors of the form $(0, 0, G_z)$. The interacting response function has been calculated solving the discretized Dyson equation [18] using the potential $v^{coul}(z, z') = -2\pi|z - z'|$. In Fig. (1) we report the macroscopic average of the density response function, calculated within the mixed-space approach for the silicon slab (orange line):

$$\langle \chi \rangle = \frac{1}{L_{supercell}} \int dz dz' e^{-iq_z z} \chi(z, z') e^{iq_z z'}$$

The peak of the density response function is located at ~ 17 eV, like for the bulk silicon (blue dashed). This leads us to calculate the dielectric function using a similar procedure as for the bulk:

$$\varepsilon_{M,\perp} = \frac{\langle E_{\perp}^{ext} \rangle}{\langle E_{\perp}^{ext} \rangle + \langle E_{\perp}^{ind} \rangle} = \frac{1}{1 + \frac{\langle E_{\perp}^{ind} \rangle}{\langle E_{\perp}^{ext} \rangle}} \quad (12)$$

where $\langle E_{\perp}^{ext} \rangle$ and $\langle E_{\perp}^{ind} \rangle$ are respectively the macroscopic averages of the external and the induced electric fields.

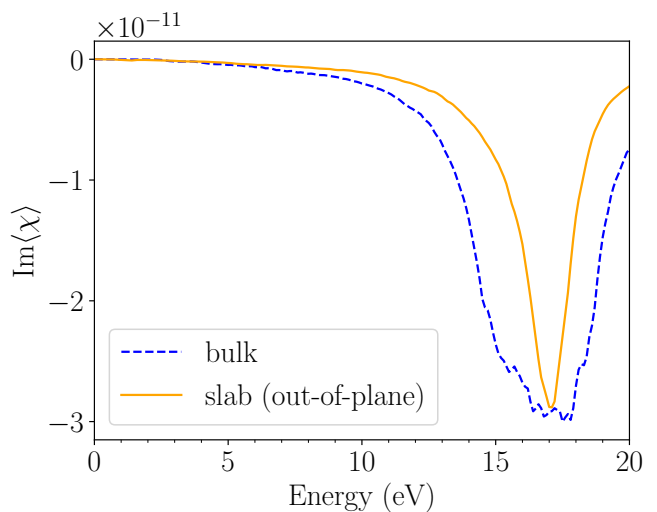


FIG. 1: Macroscopic average of the density response function of silicon (out-of-plane perturbation) for a slab (orange) and the bulk (dashed blue).

The induced field can be derived from the interacting response function. Let us suppose that the slab is perturbed by an external field directed orthogonally to the surface, of infinite wavelength, oscillating in time at frequency ω :

$$v^{ext}(z, t) = v^{ext}(z, \omega) e^{i\omega t} = z e^{i\omega t}$$

It results that:

$$E_{\perp}^{ext}(z, \omega) = -\frac{\partial}{\partial z} v^{ext}(z, \omega) = -1$$

The density variation and induced electric field are obtained according to:

$$\delta\rho(z, \omega) = \int dz' \chi(z, z', \omega) v^{ext}(z', \omega)$$

and:

$$E_{\perp}^{ind}(z, \omega) = -\frac{\partial}{\partial z} \int dz' v^{coul}(z, z') \delta\rho(z', \omega)$$

These two quantities are plotted in Fig. (2). The induced density (red solid line) exhibits a charge accumulation of opposite sign on the surfaces, while the induced electric field (blue dashed line) is roughly uniform and constant inside the slab, while it is zero outside, as expected for a slab perturbed perpendicularly to the surface.

To evaluate expression (12), one needs to perform the macroscopic average of fields, namely integrate them on a given space region and divide by the size of the integration range. It is trivial for the external macroscopic field ($\langle E_{\perp}^{ext} \rangle = -1$). Since E_{\perp}^{ind} is not uniform in space, to accomplish the average operation, the interval where the integration is performed has to be established:

$$\langle E_{\perp}^{ind} \rangle = \frac{1}{L_{mat}} \int_{-L_{mat}/2}^{L_{mat}/2} dz' E_{\perp}^{ind}(z', \omega) \quad (13)$$

¹ In this condition, Eq. (9) of Ref. 18 allows us to recover the absorption spectrum for the in-plane and out-of-plane directions (Fig. (3)). The Adler and Wiser formula is valid provided the thickness of the slab is defined to the atomic positions, which corresponds to the value used in [18]. In this former work, this was achieved by normalizing χ^0 by the factor $L_{mat}/L_z^{supercell}$, where L_{mat} was defined with the atomic positions (~ 40 bohrs).

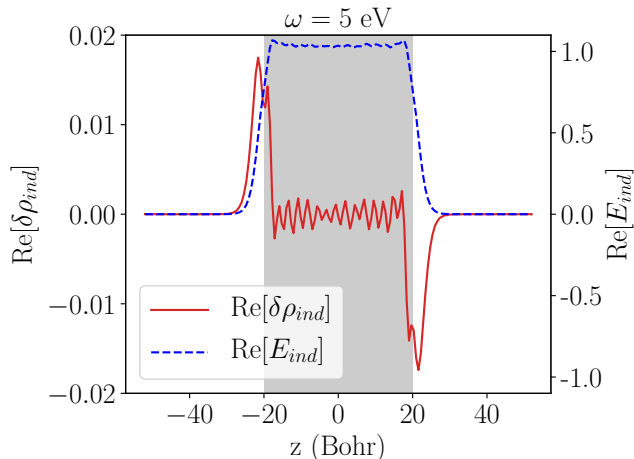


FIG. 2: Profile (real part) of the induced density (red) and electric field (dashed blue) for a silicon slab (out-of-plane perturbation of infinite wavelength and frequency: $\omega = 5$ eV).

In Fig. (3), we report several calculations of the dielectric functions (Eq. (12)), for different choices of the interval L_{mat} used to average the induced field. When we consider the whole supercell ($L_{mat} = 104$ bohrs, Fig. (3) - orange crosses), we obtain the same result as the standard supercell approach, (i.e., in reciprocal space using the 3D Coulomb potential,) which corresponds to an effective medium theory with vacuum [18].

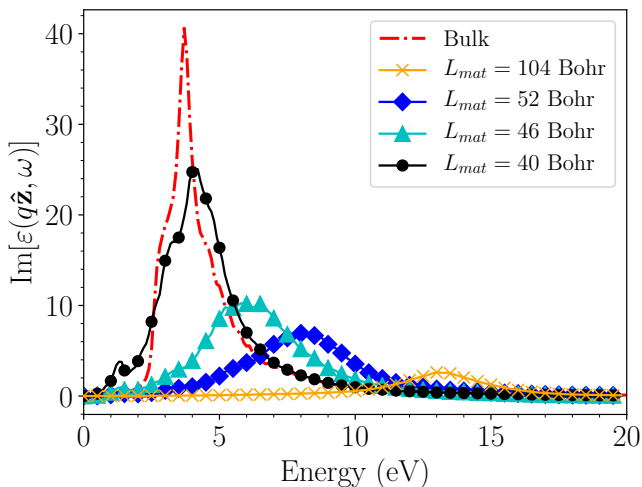


FIG. 3: Imaginary part of the out-of-plane component of the dielectric function for several integration domains for E_{\perp}^{ind} (Eq. (13)).

Reducing the interval (Fig. (3)), the absorption peak shifts toward lower energies and its amplitude increases as for EMT. The reduction of $\langle E_{\perp}^{ind} \rangle$ does not compensate the reduction of the length of integration L_{mat} . When we take $L_{mat} = 40$ bohrs (gray region of Fig.

(2)), corresponding to the atomic positions of the top most and bottom most layers (Fig. (3), black circles) the absorption peak is situated at 4 eV like in the bulk silicon spectrum (Fig. (3), red dashed dotted). One notes that we also recover the spectrum of the right panel of Fig. (4) of Ref. 18, where the value of L_{mat} was also 40 bohrs. Even if it is meaningless to integrate up to 104 bohrs, since we obviously include vacuum, the problem appears critical in the region between 52 and 40 bohrs (Figs. (3) and (2)). The question which arises naturally is how to define the thickness of the matter, since the region where $\delta\rho(z, \omega) \neq 0$ (and the induced field as well) is quite larger than the region defined by surface atomic layers (Fig. (2)). A similar finding has been reported for surfaces [39, 40] and 2D objects [41, 42]. Equation (7) would also give similar results. For $L_{mat} \sim 52$ bohrs, where the induced density and electric field reach zero, the peak is located at ~ 8 eV (Fig. (3) - blue diamonds). This is what we call "the L_{mat} problem": there is not a clear way to define the slab thickness, and this uncertainty affects in a dramatic way the calculation of the dielectric function, making in practice ambiguous the calculation of the absorption spectrum with the Adler and Wiser formula.

D. In-plane response

We computed the independent particle response function in the reciprocal space for $\mathbf{q} = q\hat{\mathbf{x}}$ (in-plane direction), in the optical limit ($|\mathbf{q}| = 10^{-5}$ bohrs $^{-1}$). We solved the discretized Dyson equation ([18]) with the potential defined in Eq. (11) to find the interacting response function of the isolated slab. We want to use this quantity to obtain the macroscopic dielectric function. In the case of a infinite and periodic material, the standard procedure is to calculate the inverse dielectric function (Eq. (1)) and obtain the macroscopic dielectric function according to Eq. (2), which can be rewritten as:

$$\varepsilon_M = \frac{1}{\varepsilon_{\mathbf{00}}^{-1}} = \frac{v_{\mathbf{0}}^{ext}}{v_{\mathbf{0}}^{tot}} \quad (14)$$

In analogy with Eqs. (1) and (14), we evaluated the microscopic inverse dielectric function:

$$\varepsilon^{-1}(\mathbf{q}_{\parallel}, z_i, z_j; \omega) = \frac{\delta_{ij}}{\Delta_z} + \sum_l v^{coul}(z_i, z_l) \chi(\mathbf{q}_{\parallel}, z_l, z_j; \omega) \Delta_z$$

and we extracted its macroscopic average:

$$\langle \varepsilon^{-1} \rangle(\mathbf{q}, \omega) = \frac{1}{L_{SC}} \sum_{ij} e^{-iq_z z_i} \varepsilon^{-1}(\mathbf{q}_{\parallel}, z_i, z_j; \omega) e^{iq_z z_j} \Delta_z^2 \quad (15)$$

Finally, we calculated:

$$\frac{1}{\langle \varepsilon^{-1} \rangle}(\mathbf{q}, \omega) \quad (16)$$

The result of this calculation is shown in Fig. (4): it has a peak at 4 eV (like bulk silicon), but, compared to the dielectric function of bulk silicon (Fig. (3) - red dashed dotted), it is suppressed of about four order of magnitude. The real part is ≈ 1 , while the imaginary part is almost zero.

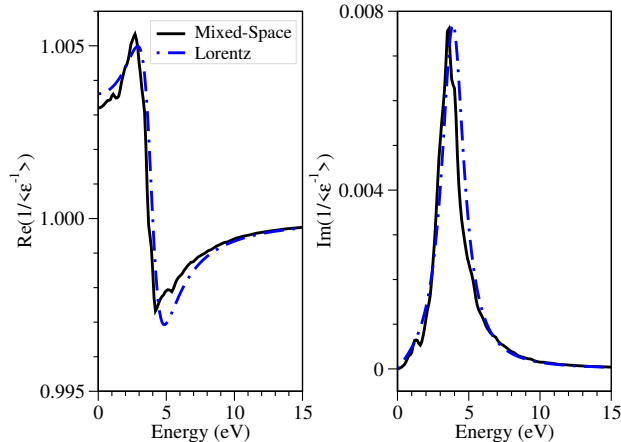


FIG. 4: In-plane dielectric function of the silicon slab calculated according Eqs. (15) and (16) (solid black) or Eqs. (38) and (39) (dashed blue).

The quantity calculated according to Eq. (16) (Fig. (4)) actually corresponds to the result of Eq. (3) ([20]). Moreover, the result is proportional to $|\mathbf{q}|$.

In Sec. III C, we will explain the physical meaning of this behaviour, and demonstrate that the in-plane dielectric function is (Eq. (45)):

$$\varepsilon_{M,\parallel} = 1 - \frac{4\pi}{|\mathbf{q}|^2} \langle \chi \rangle \quad (17)$$

where:

$$\langle \chi \rangle = \frac{1}{L_{mat}} \int dz \int dz' \chi(\mathbf{q}_{\parallel}, z, z') \quad (18)$$

This procedure is similar to Eq. (4), and it would give the same spectra, provided L_{mat} and d are equal. The spectrum calculated with Eq. (17) and (18) is reported in Fig. (5) for different values of L_{mat} : the correct order of magnitude for the amplitude is recovered, contrarily to Fig. (4). Choosing $L_{mat} = 40$ bohrs (distance between the interfacial atomic planes of the slab), we recover the amplitude of the bulk silicon (Fig. (5) - red dashed dotted). Due to the fact that the $\chi(z, z')$ goes rapidly to zero out of the region occupied by atoms, the integration is independent on the choice of L_{mat} , so the definition of the thickness of the matter just acts as a scaling factor, contrarily to out-of-plane component (Fig. (3)). Nevertheless, even in the case of in-plane perturbation, the uncertainty on the thickness L_{mat} affects the definition of the dielectric function.

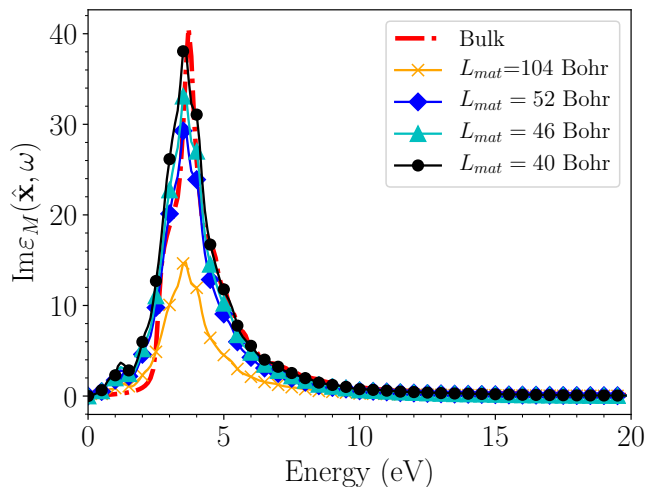


FIG. 5: Imaginary part of the in-plane components of the dielectric function for $\langle \chi \rangle$ (Eq. (17) and (18)).

III. LORENTZ MODEL

We have established that the response function of an isolated thin slab exhibits two peaks: the first one appears for an in-plane excitation and is located at the resonance of absorption of the bulk material, and the second one, resulting from an out-of-plane perturbation is located at the plasmon frequency of the bulk material. The relation between the density response function and the optical response of a thin slab appears completely different from the one of the infinite 3D crystal. To clarify this puzzling result, we propose to approach the problem within a simple Lorentz oscillators model, where electrons are depicted as n_e classical oscillators per unit of volume having charge e and mass m_e , bound to the nuclei by an elastic force of frequency ω_0 . We consider an external longitudinal perturbation of the form:

$$\mathbf{E}^{ext}(\mathbf{r}, t) = \mathbf{E}_0^{ext} e^{i\mathbf{q}\cdot\mathbf{r} - i\omega t}$$

The displacement of the oscillator in \mathbf{r} at time t is given by the vector field $\mathbf{\Delta}(\mathbf{r}, t)$. Each oscillator feels an harmonic force $-m_e\omega_0^2\mathbf{\Delta}$, a dampening force $-(m_e/\tau)\dot{\mathbf{\Delta}}$, and the electrostatic forces given by the external and induced electric fields. The equation of motion reads:

$$m_e \ddot{\mathbf{\Delta}}(\mathbf{r}, t) = -m_e\omega_0^2\mathbf{\Delta}(\mathbf{r}, t) - \frac{m_e}{\tau}\dot{\mathbf{\Delta}}(\mathbf{r}, t) + e\mathbf{E}^{ext}(\mathbf{r}, t) + e\mathbf{E}^{ind}(\mathbf{r}, t) \quad (19)$$

The polarization density is expressed as:

$$\mathbf{P}(\mathbf{r}, t) = n_e e \mathbf{\Delta}(\mathbf{r}, t)$$

and the induced charge density:

$$\rho^{ind}(\mathbf{r}, t) = -\nabla \cdot \mathbf{P}(\mathbf{r}, t)$$

In appendix (A), we summarised the results for the infinite material to allow the comparison with the slab.

A. In-plane perturbation

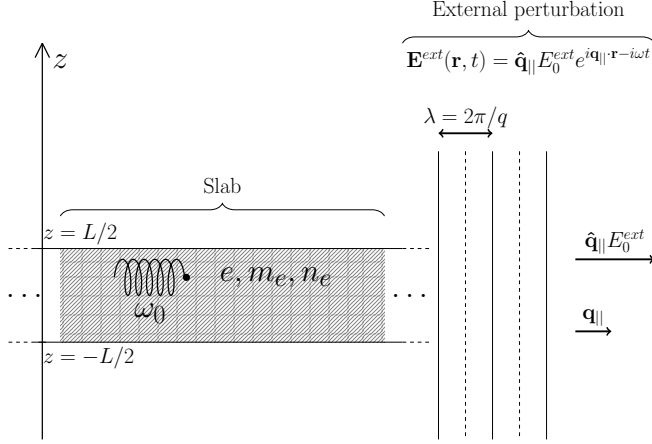


FIG. 6: Slab undergoing an external longitudinal perturbation of wave vector \mathbf{q} and frequency ω , with the electric field parallel to the surface.

We consider an external longitudinal perturbation having the field parallel to the surface:

$$\mathbf{E}^{ext} = \mathbf{E}_0 e^{i\mathbf{q}_{\parallel} \cdot \mathbf{r} - i\omega t}$$

with \mathbf{q}_{\parallel} and \mathbf{E}_0 are chosen along $\hat{\mathbf{x}}$ (Fig. (6)). We search for a solution of the form:

$$\Delta(\mathbf{r}, t) = \Theta(z + \frac{L}{2})\Theta(-z + \frac{L}{2})\Delta_0 e^{i\mathbf{q}_{\parallel} \cdot \mathbf{r} - i\omega t} \quad \text{with } \Delta_0 \parallel \hat{\mathbf{x}}$$

which implied a polarization density:

$$\mathbf{P}(\mathbf{r}, t) = en_e \Theta(z + \frac{L}{2})\Theta(-z + \frac{L}{2})\Delta_0 e^{i\mathbf{q}_{\parallel} \cdot \mathbf{r} - i\omega t} \quad (20)$$

Such a charge distribution induces an electrostatic potential (see App. B):

$$\phi^{ind}(\mathbf{r}, t) = -\frac{4\pi}{|q_{\parallel}|^2} ien_e q_{\parallel} F(z) \Delta_0 e^{i\mathbf{q}_{\parallel} \cdot \mathbf{r} - i\omega t}$$

where $F(z)$ is:

$$F(z) = \begin{cases} e^{-|q_{\parallel}|z} \sinh(|q_{\parallel}|L/2) & \text{for } z > L/2 \\ \left[1 - e^{-|q_{\parallel}| \frac{L}{2}} \cosh(|q_{\parallel}|z) \right] & \text{for } z \in [-\frac{L}{2}, \frac{L}{2}] \\ e^{|q_{\parallel}|z} \sinh(|q_{\parallel}|L/2) & \text{for } z < -L/2 \end{cases}$$

The in-plane component of the induced electric field is given by:

$$E_x^{ind}(\mathbf{r}, t) = -\frac{\partial}{\partial x} \phi^{ind}(\mathbf{r}, t) = -4\pi en_e F(z) \Delta_0 e^{i\mathbf{q}_{\parallel} \cdot \mathbf{r} - i\omega t} \quad (21)$$

and the component of the induced electric field orthogonal to the surface by:

$$\begin{aligned} E_z^{ind}(\mathbf{r}, t) &= -\frac{\partial}{\partial z} \phi^{ind}(\mathbf{r}, t) \\ &= \frac{1}{|q_{\parallel}|} 4\pi in_e e \left(\frac{\partial}{\partial z} F(z) \right) \Delta_0 e^{i\mathbf{q}_{\parallel} \cdot \mathbf{r} - i\omega t} \end{aligned} \quad (22)$$

Let us consider the expression of the induced electric field (Eqs. (21) and (22)) in two limits:

1. $|q_{\parallel}| \frac{L}{2} \gg 1$ (thickness much greater than the perturbation wavelength). The induced field inside the slab, far from the surfaces ($|z| \ll L$) is:

$$E_x^{ind}(\mathbf{r}, t) \xrightarrow{|q_{\parallel}| \frac{L}{2} \gg 1} -4\pi n_e e \Delta_0 e^{i\mathbf{q}_{\parallel} \cdot \mathbf{r} - i\omega t} \quad (23)$$

$$E_z^{ind}(\mathbf{r}, t) \xrightarrow{|q_{\parallel}| \frac{L}{2} \gg 1} 0 \quad (24)$$

We recover the electric field induced in a bulk (Eq. (A2)).

2. $|q_{\parallel}| \frac{L}{2} \ll 1$ (limit of thickness much smaller than the perturbation wavelength)². The induced electric field inside the slab is:

$$E_x^{ind}(\mathbf{r}, t) \xrightarrow{|q_{\parallel}| \frac{L}{2} \ll 1} -4\pi n_e e q_{\parallel} \frac{L}{2} \Delta_0 e^{i\mathbf{q}_{\parallel} \cdot \mathbf{r} - i\omega t} \quad (25)$$

$$E_z^{ind}(\mathbf{r}, t) \xrightarrow{|q_{\parallel}| \frac{L}{2} \ll 1} -i4\pi n_e e |q_{\parallel}| z \Delta_0 e^{i\mathbf{q}_{\parallel} \cdot \mathbf{r} - i\omega t} \quad (26)$$

We evidence that the electric field induced inside a thin slab is, with respect to the case of the bulk, smaller of a factor $(|q_{\parallel}|L/2)$. This implies that

$$E_z^{ind}, E_x^{ind} \sim |q_{\parallel}|L/2 \ll |\mathbf{E}^{ext}| \quad (27)$$

and justifies the guess $\Delta(\mathbf{r}, t) \parallel \mathbf{q}$.

The induced field is strongly depressed compared to the bulk case due to the long-range and non-local nature of the Coulomb interaction. Most of charges contributing to the potential inside the slab are suppressed when the two parallel half spaces are cut away to define the slab. In the following, we will focus on the limit $|q_{\parallel}| \frac{L}{2} \ll 1$. Using Eq. (25), we can solve the equation of motion and express the displacement of oscillators as a function of the external field:

$$\Delta_0 = \frac{e}{m_e - \omega^2 + \omega_0^2 - i\frac{\omega}{\tau} + \omega_{pl}^2 |q_{\parallel}| \frac{L}{2}} \mathbf{E}_0^{ext} \quad (28)$$

leading to the response function of density (Fig. (7)):

$$\chi = \frac{|q_{\parallel}|^2}{4\pi} \frac{\omega_{pl}^2}{\omega^2 - \omega_0^2 + i\frac{\omega}{\tau} - \frac{|q_{\parallel}|L}{2} \omega_{pl}^2} \quad (29)$$

² Corresponding to our *ab initio* calculation

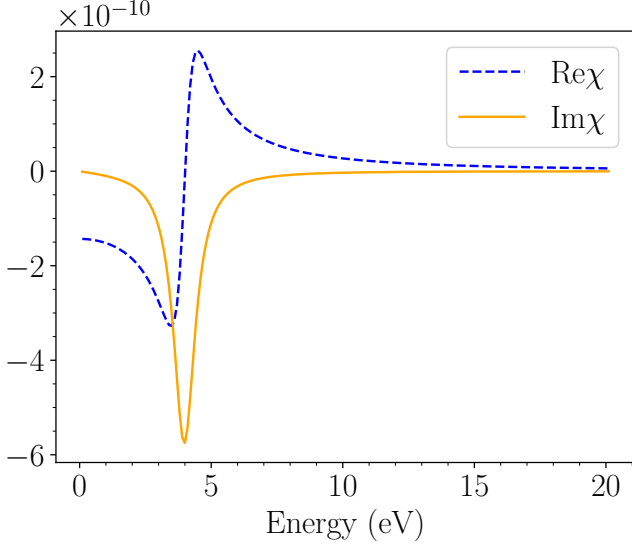


FIG. 7: Density response function of the slab within the Lorentz model (for an in-plane perturbation of long wavelength).

It presents a significant difference as compared to its bulk counterpart (Eq. (A4)). Contrarily to the case of the bulk, the maximum of this quantity is located at:

$$\sqrt{\omega_0^2 + |q_{||}| \frac{L}{2} \omega_{pl}^2} \approx \omega_0$$

The electrons behave as independent particles. The displacement of oscillators can be recasted as a function of the total field:

$$\Delta(\mathbf{r}, t) = \frac{e}{m_e} \Theta(z + \frac{L}{2}) \Theta(-z + \frac{L}{2}) \frac{1}{-\omega^2 + \omega_0^2 - i \frac{\omega}{\tau}} \mathbf{E}^{tot}(\mathbf{r}, t) \quad (30)$$

to get the conductivity and the dielectric function (see Section III C).

B. Out-of-plane perturbation

Let us consider a slab undergoing an external perturbation of infinite wavelength orthogonal to the surface (Fig. (8a)):

$$\mathbf{E}^{ext}(\mathbf{r}, t) = \mathbf{E}_0^{ext} e^{-i\omega t} \quad \text{with} \quad \mathbf{E}_0^{ext} \parallel \hat{\mathbf{z}}$$

We make a guess on the functional form of $\Delta(\mathbf{r}, t)$:

$$\Delta(\mathbf{r}, t) = \Theta(z + \frac{L}{2}) \Theta(-z + \frac{L}{2}) \Delta_0 e^{-i\omega t} \quad \text{with} \quad \Delta_0 \parallel \hat{\mathbf{z}}$$

where Θ is the Heaviside function, which means that the displacement of oscillators is uniform on the slab, and zero outside. The polarization density is:

$$\mathbf{P}(\mathbf{r}, t) = n_e e \Theta(z + \frac{L}{2}) \Theta(-z + \frac{L}{2}) \Delta_0 e^{-i\omega t}$$

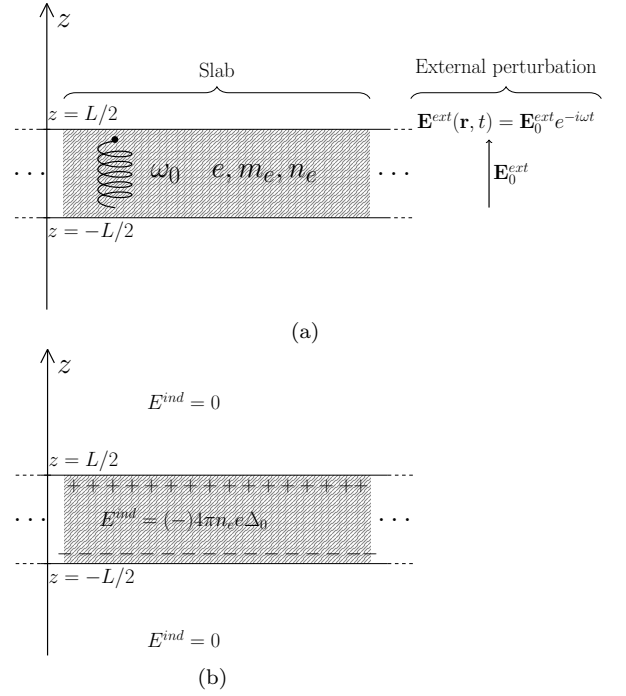


FIG. 8: (a): slab undergoing an external electric perturbation of infinite wavelength orthogonal to the surface. (b): accumulation of charges of opposite sign, resulting in an induced electric field uniform and constant inside the slab, and zero outside.

The induced density is

$$\rho^{ind}(\mathbf{r}, t) = -n_e e \Delta_0 e^{-i\omega t} \left(\delta(z + \frac{L}{2}) - \delta(-z + \frac{L}{2}) \right)$$

As expected, the induced density of charge of a slab in an external field of infinite wavelength orthogonal to the surface is constituted by two planar distribution of opposite sign located on the faces of the slab (Fig. (8b)). Such a charge distribution induces the electrostatic potential:

$$\begin{aligned} \phi^{ind}(z, t) &= - \int dz' 2\pi |z - z'| \rho^{ind}(z', t) = \\ &= 2\pi n_e e \Delta_0 e^{-i\omega t} \left(|z + \frac{L}{2}| - |z - \frac{L}{2}| \right) \\ &= 2\pi n_e e \Delta_0 e^{-i\omega t} \begin{cases} L & \text{for } z > L/2 \\ 2z & \text{for } -L/2 < z < L/2 \\ -L & \text{for } z < -L/2 \end{cases} \end{aligned}$$

leading to the induced electric field:

$$\mathbf{E}^{ind}(\mathbf{r}, t) = -4\pi n_e e \Theta(z + \frac{L}{2}) \Theta(-z + \frac{L}{2}) \Delta_0 e^{-i\omega t} \quad (31)$$

\mathbf{E}^{ind} is parallel to Δ_0 which justify the guess $\Delta_0 \parallel \hat{\mathbf{z}}$. It is zero outside the slab, while inside, it is uniform and homogeneous. We recover the results obtained within the mixed-space approach for the out-of-plane perturbation

(Fig. (2)). This corresponds to the known case of a capacitor in an electric field perpendicular to the slab. One notes that the value of the induced field inside the slab is equal to the one of the bulk. Surprisingly, it is in the direction where the matter has been cut that we recover the bulk result. Using the relation between the displacement and the induced electric field, we obtain the relation between the displacement and the external electric field:

$$\Delta_0 = \frac{e}{m_e} \frac{1}{-\omega^2 + \omega_0^2 - i\frac{\omega}{\tau} + \omega_{pl}^2} \mathbf{E}_0^{ext} \quad (32)$$

and the relation between the displacement and the total electric field :

$$\Delta(\mathbf{r}, t) = \frac{e}{m_e} \Theta(z + \frac{L}{2}) \Theta(-z + \frac{L}{2}) \frac{1}{-\omega^2 + \omega_0^2 - i\frac{\omega}{\tau}} \mathbf{E}^{tot}(\mathbf{r}, t) \quad (33)$$

which will allows us to derive the dielectric function.

C. Dielectric function

From Eqs. (33) and (30) we can express the current density $\mathbf{J}(\mathbf{r}, t)$ as a function of the total electric field to extract the conductivity:

$$\sigma(\omega) = \frac{1}{4\pi} \frac{i\omega\omega_{pl}^2}{\omega^2 - \omega_0^2 + i\frac{\omega}{\tau}} \quad (34)$$

and the dielectric function, via the expression (A6):

$$\varepsilon(\omega) = 1 - \frac{\omega_{pl}^2}{\omega^2 - \omega_0^2 + i\frac{\omega}{\tau}} \quad (35)$$

Surprisingly, despite the important differences in the response of the slab according to the direction of the perturbation (Eqs. (32) and (28)), the dielectric function is the same. The relation between the dielectric function and the density response function depends on the direction of the perturbation. This relation is typically expressed by Eq. (14). This equation is written in reciprocal space, and refers to systems which are periodic. This is not the case for the slab of oscillators depicted in Figs. (8) and (6) which are finite and isolated in the out-of-plane direction, making definition of cell-averaged quantities meaningless. We propose to calculate the dielectric function in analogy with Eq. (14), replacing the cell averaged quantities with the fields averaged *over the slab*³:

$$\varepsilon_M = \frac{\langle E_{\perp}^{ext} \rangle_{slab}}{\langle E_{\perp}^{ext} \rangle_{slab} + \langle E_{\perp}^{ind} \rangle_{slab}} \quad (36)$$

³ here $\langle \cdot \rangle_{slab}$ stand for:

$$\langle f(z) \rangle_{slab} = \frac{1}{L} \int_{-L/2}^{L/2} f(z) dz$$

Replacing in Eq. (36) the induced field reported in Eq. (31), one obtains:

$$\varepsilon_M = \frac{\langle E_{\perp}^{ext} \rangle_{slab}}{\langle E_{\perp}^{ext} \rangle_{slab} + \langle E_{\perp}^{ind} \rangle_{slab}} = 1 - \frac{\omega_{pl}^2}{\omega^2 - \omega_0^2 + i\frac{\omega}{\tau}} \quad (37)$$

and the result reported in Eq. (35) is recovered. The case of the in-plane component is more puzzling. Replacing Eq. (21) in (36), one obtains:

$$\varepsilon_M = \frac{\langle E_{\parallel}^{ext} \rangle_{slab}}{\langle E_{\parallel}^{ext} \rangle_{slab} + \langle E_{\parallel}^{ind} \rangle_{slab}} \quad (38)$$

which in the limit $q_{\parallel}L/2 \ll 1$ reduces to:

$$\frac{\langle E_{\parallel}^{ext} \rangle_{slab}}{\langle E_{\parallel}^{ext} \rangle_{slab} + \langle E_{\parallel}^{ind} \rangle_{slab}} \approx 1 - \frac{|q_{\parallel}|L}{2} \frac{\omega_{pl}^2}{\omega^2 - \omega_0^2 + i\frac{\omega}{\tau}} \quad (39)$$

We reported this result in Fig. (4) (dashed blue). The dielectric function calculated according formula (38) has real part ≈ 1 and imaginary part ≈ 0 . This feature is similar to the one calculated within the mixed-space framework with Eq. (15) (Fig. (4) - black line). Eq. (39) allows us to interpret this result: it is a consequence of the strong reduction of the induced field occurring in the limit of thin slab. We stress out that, since the induced field has been averaged *over the slab*, this result cannot come from an effective medium theory with vacuum, but it is a real physical effect due to the reduced size of the slab. The situation is quite confusing: the dielectric function calculated through the conductivity (Eq. (35)) and the one calculated by mean of formula (38) depict totally different physics due to the $|q_{\parallel}|L/2$ prefactor. The last part of the present section will be devoted to elucidate this point.

The macroscopic dielectric function is defined as the quantity which relates the electric displacement \mathbf{D} with the electric field \mathbf{E} :

$$\mathbf{D} = \overset{\leftrightarrow}{\varepsilon}_M \mathbf{E} \quad (40)$$

where the electric displacement \mathbf{D} is defined by the constitutive relation:

$$\mathbf{D} = \mathbf{E} + 4\pi\mathbf{P} \quad (41)$$

When an infinite material undergoes a longitudinal external perturbation, the induced electric field and the polarization of the system are linked by the following relation [27]:

$$\mathbf{E}^{ind} = -4\pi\mathbf{P} \quad (42)$$

From the latter equation and the constitutive relation (41), it follows that:

$$\mathbf{D} = \mathbf{E}^{ext} \quad (43)$$

Putting Eq. (43) in (40), we immediately obtain:

$$\varepsilon_M = \frac{E^{ext}}{E^{ext} + E^{ind}}$$

However, the comparison of Eqs. (21) and (20) shows that for an in plane perturbation in a thin slab:

$$-4\pi\mathbf{P} \neq \mathbf{E}^{ind} \quad \Rightarrow \quad \mathbf{D} \neq \mathbf{E}^{ext}$$

and therefore Eqs. (42) and (43) are no more valid in the case of a 2D system. Moreover, one can show that \mathbf{P} is no more purely longitudinal, contrarily to the induced field \mathbf{E}^{ind} (see Appendix C). So we have:

$$\mathbf{D}_L + \mathbf{D}_T = \mathbf{E}_L^{ext} + \mathbf{E}_L^{ind} + 4\pi\mathbf{P}_L + 4\pi\mathbf{P}_T$$

The fact that a purely longitudinal perturbation induces also a transverse polarization may be source of perplexity. However, it has been already reported by Del Sole and E. Fiorino [43] that for infinite materials of cubic symmetry, a longitudinal perturbation always produces a purely longitudinal response, but this is no more valid when non-cubic symmetry is considered, or when interfaces are to take in account. We show it explicitly in Eq. (C1) for the latter case.

However, the constitutive equation (41) is still valid, and (assuming the diagonality of the tensor) the in-plane component may be obtained as:

$$\varepsilon_{M,\parallel} = \frac{\langle E_{\parallel}^{ext} \rangle_{slab} + \langle E_{\parallel}^{ind} \rangle_{slab} + 4\pi\langle P_{\parallel} \rangle_{slab}}{\langle E_{\parallel}^{ext} \rangle_{slab} + \langle E_{\parallel}^{ind} \rangle_{slab}} \quad (44)$$

In the limit of thick slab (Eq. (23)), the induced field approaches the bulk result, the condition (42) is recovered, and equation (44) becomes:

$$\begin{aligned} \varepsilon_{M,\parallel} &\xrightarrow{|q_{\parallel}| \frac{L}{2} \gg 1} \frac{\langle E_{\parallel}^{ext} \rangle_{slab} + \cancel{\langle E_{\parallel}^{ind} \rangle_{slab}} + \cancel{4\pi\langle P_{\parallel} \rangle_{slab}}}{\langle E_{\parallel}^{ext} \rangle_{slab} + \langle E_{\parallel}^{ind} \rangle_{slab}} \\ &= \frac{\langle E_{\parallel}^{ext} \rangle_{slab}}{\langle E_{\parallel}^{ext} \rangle_{slab} + \langle E_{\parallel}^{ind} \rangle_{slab}} \end{aligned}$$

We re-obtain the expression valid for the infinite material.

In the limit of thin slab, the induced field becomes negligible as compared to the external one, and we have:

$$\begin{aligned} \varepsilon_{M,\parallel} &\xrightarrow{|q_{\parallel}| \frac{L}{2} \ll 1} \frac{\langle E_{\parallel}^{ext} \rangle_{slab} + \cancel{\langle E_{\parallel}^{ind} \rangle_{slab}} + 4\pi\langle P_{\parallel} \rangle_{slab}}{\langle E_{\parallel}^{ext} \rangle_{slab} + \cancel{\langle E_{\parallel}^{ind} \rangle_{slab}}} \\ &= 1 + 4\pi \frac{\langle P_{\parallel} \rangle_{slab}}{\langle E_{\parallel}^{ext} \rangle_{slab}} \end{aligned}$$

Exploiting the relation between polarization and induced charge density we can express P_{\parallel} as:

$$iq_{\parallel}P_{\parallel} = \frac{1}{iq_{\parallel}}\chi E^{ext}$$

so that we obtain:

$$\varepsilon_{M,\parallel} \xrightarrow{|q_{\parallel}| \frac{L}{2} \ll 1} 1 - \frac{4\pi}{q_{\parallel}^2} \langle \chi \rangle \quad (45)$$

This proves that Eq. (45) should be used to calculate in-plane optical properties of thin films and 2D systems. The spectra calculated with Eq. (45), where $\langle \chi \rangle$ has been obtained within mixed-space approach (see Sec. IID), have been presented in Fig. (5). We have evidenced that the expected amplitude was recovered.

In conclusion, we elucidated the differences between the response of the slab and a bulk system to an external longitudinal perturbation, for both in- and out-of-plane perturbations. The most puzzling result concerns the in-plane case. The correct relationship to calculate the dielectric function is Eq. (44). In the case of a bulk, it is equivalent to Eq. (38), and one recovers the well known result that for bulk cubic materials, in the optical limit, the longitudinal-longitudinal component of the dielectric function can be used to calculate the transverse-transverse one, leading to absorption [13–15]. For the slab, the presence of a transverse polarization implies that one should apply Eq. (44). Even if it is not trivial to identify the components of the dielectric tensor, in the limit of thin slab, Eq. (44) reproduces the expression commonly admitted to describe absorption of 2D systems, and that we have demonstrated in Eq. (45). We believe that a key role in reproducing such result is played by the inclusion of the transverse part of the polarization.

IV. LINK WITH THE EXPERIMENT: REFLECTANCE AND TRANSMITTANCE

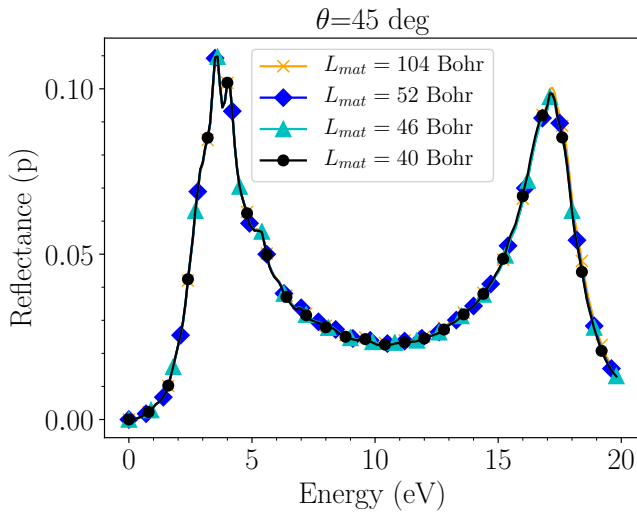
As we have seen in the previous sections, the spectral weight of the ε_M , and specially for the out-of-plane component, is strongly affected by the definition of the thickness of the matter. In order to understand which physics could be contained in these quantities, we propose to study numerically the reflectance and transmittance as optical observables. Using a transfer matrix formalism for a slab of biaxial material in vacuum [44]⁴, we express the reflection and transmission coefficients. For p polarization (which allows the presence of a component of the electric field perpendicular to the surface), we get:

⁴ For one isotropic film, the matrix transfer formalism reproduces the well-known Airy's formulas [45–48].

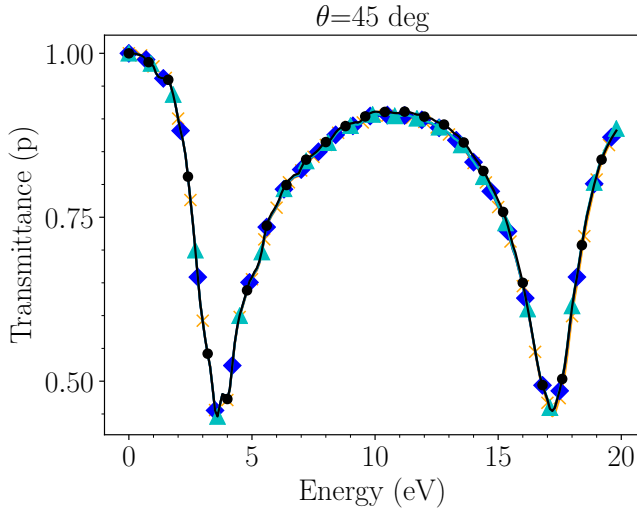
$$r_{pp} = \frac{i \sin(\kappa_p) \left[1 - 1/\varepsilon_{\perp} \sin^2(\theta) - \varepsilon_{\parallel} \cos^2(\theta) \right]}{2 \sqrt{\varepsilon_{\parallel}} \sqrt{1 - [1/\varepsilon_{\perp} \sin^2(\theta)]} \cos(\kappa_p) \cos(\theta) - i \sin(\kappa_p) \left[1 - 1/\varepsilon_{\perp} \sin^2(\theta) + \varepsilon_{\parallel} \cos^2(\theta) \right]} \quad (46)$$

$$t_{pp} = \frac{2 \sqrt{\varepsilon_{\parallel}} \sqrt{1 - [1/\varepsilon_{\perp} \sin^2(\theta)]} \cos(\theta)}{2 \sqrt{\varepsilon_{\parallel}} \sqrt{1 - [1/\varepsilon_{\perp} \sin^2(\theta)]} \cos(\kappa_p) \cos(\theta) - i \sin(\kappa_p) \left[1 - 1/\varepsilon_{\perp} \sin^2(\theta) + \varepsilon_{\parallel} \cos^2(\theta) \right]} \quad (47)$$

with $\kappa_p = \frac{\omega}{c} L_{mat} \sqrt{\varepsilon_{\parallel}} \sqrt{1 - [1/\varepsilon_{\perp} \sin^2(\theta)]}$



(a)



(b)

FIG. 9: (a): Reflectance $|r_{pp}|^2$ (Eq. (46)) and (b): Transmittance $|t_{pp}|^2$ (Eq. (47)) for anisotropic dielectric functions of Figs. (5) and (3).

As ε_{\parallel} and ε_{\perp} in Eqs. (46) and (47) we use the spectra presented in Figs. (5) and (3) associated to the same L_{mat} . The reflectance $|r_{pp}|^2$ and transmittance $|t_{pp}|^2$ spectra are shown in Fig. (9) for an incident angle of $\theta = 45$ deg. All the spectra calculated using the different $\varepsilon_{M,\parallel}$ and $\varepsilon_{M,\perp}$ each associated with the corresponding L_{mat} , are similar. This interesting and somehow comforting result show that the ambiguity on the definition of the thickness of matter has no consequence on the observables which should be measured in an optical experiment. This observation leads to the important conclusion that any value of L_{mat} can be used when the calculation of these quantities is under concern. Moreover, it confirms that the quantities calculated within the longitudinal formalism of TD-DFT can still be used to extract the optical response for a thin slab.

V. CONCLUSION

In this paper, we showed that the Adler and Wiser formula which, in 3D systems, allows the calculation of the absorption spectrum, cannot be used for a very thin object. For a longitudinal perturbation parallel to the plane, the integration of $\varepsilon^{-1}(z, z')$ on a range corresponding to the limit where the induced density reaches zero gives a non-local quantity, almost equal to 1, depicting the screening. In this case, the Adler and Wiser formula gives an absorption spectrum under-evaluated of several order of magnitude, and $|\mathbf{q}|$ -dependent (Fig. (4)). Thanks to the Lorentz model, we evidenced that the induced electric field is strongly reduced, and the polarization contains a transverse part. This allows us to demonstrate that the macroscopic dielectric tensor, leading to the absorption spectrum, is proportional to the macroscopic response function $\chi(\mathbf{q}_{\parallel})$ of the isolated slab (Eq. (45)). It presents a resonance at the absorption frequency of the bulk counterpart (Fig. (5)). For an out-of-plane perturbation, we showed that, due to charge accumulation on interfaces (Fig. (2)), the induced electric field and polarization are similar to the bulk ones, leading to the bulk definition of the macroscopic dielectric function. The Adler and Wiser formula seems to be valid, and one would expect a resonance at the absorption frequency of the bulk counterpart (Eq. (37)). But the result is

strongly affected by the ambiguity of the definition the thickness of the matter. Nevertheless, we showed that this so-called L_{mat} problem has no consequence on the measured optical quantities like reflectance and transmittance, in agreement with the fact that for a quasi-2D object, the physical quantities should be defined propor-

tionally to the thickness.

VI. ACKNOWLEDGMENTS

This work was granted access to the HPC/AI resources of IDRIS and TGCC under the allocation (Grant No. 0900544) made by GENCI.

Appendix A: Lorentz model: infinite system

Solution of Eq. (19) is well known for the case of an infinite system:

$$\mathbf{\Delta}(\mathbf{r}, t) = \mathbf{\Delta}_0 e^{i\mathbf{q}\cdot\mathbf{r} - i\omega t} \quad (\text{A1})$$

This displacement of electrons produces an induced field of the form:

$$\mathbf{E}^{ind} = -4\pi n_e e \mathbf{\Delta}(\mathbf{r}, t) \quad (\text{A2})$$

resulting in the following relationship between the displacement of electrons and the external field:

$$\mathbf{\Delta}_0 = \frac{e}{m_e} \frac{1}{-\omega^2 + \omega_0^2 - i\frac{\omega}{\tau} + \omega_{pl}^2} \mathbf{E}_0^{ext} \quad (\text{A3})$$

From this relation, we can extract the response function of density, which links the induced density with the external potential:

$$\chi_{\rho\rho} = \frac{|\mathbf{q}|^2}{4\pi} \frac{\omega_{pl}^2}{\omega^2 - \omega_0^2 + i\frac{\omega}{\tau} - \omega_{pl}^2} \quad (\text{A4})$$

We recover the well known result that in a bulk material, the density response function exhibit a resonance associated with the plasmon frequency: $\sqrt{\omega_0^2 + \omega_{pl}^2}$. We can rewrite the displacement of electrons as a function of the total field:

$$\mathbf{\Delta}(\mathbf{r}, t) = \frac{e}{m_e} \frac{1}{-\omega^2 + \omega_0^2 - i\frac{\omega}{\tau}} \mathbf{E}^{tot}(\mathbf{r}, t) \quad (\text{A5})$$

From this relation, we can derive an expression of the induced current as a function of the electric field:

$$\begin{aligned} \mathbf{J}^{ind}(\mathbf{r}, t) &= n_e e \dot{\mathbf{\Delta}}(\mathbf{r}, t) \\ &= \frac{1}{4\pi} \frac{i\omega\omega_{pl}^2}{\omega^2 - \omega_0^2 + i\frac{\omega}{\tau}} \mathbf{E}^{tot}(\mathbf{r}, t) \\ &= \sigma(\omega) \mathbf{E}^{tot}(\mathbf{r}, t) \end{aligned}$$

which defines the conductivity:

$$\sigma(\omega) = \frac{1}{4\pi} \frac{i\omega\omega_{pl}^2}{\omega^2 - \omega_0^2 + i\frac{\omega}{\tau}}$$

The dielectric function is obtained via the relation [49]

$$\varepsilon(\omega) = 1 + \frac{4\pi i\sigma(\omega)}{\omega} \quad (\text{A6})$$

giving

$$\varepsilon(\omega) = 1 - \frac{\omega_{pl}^2}{\omega^2 - \omega_0^2 + i\frac{\omega}{\tau}}$$

Appendix B: Potential induced in a thin slab by an in-plane perturbation

Using the expression of polarization (Eq. (20)) the induced density of charge can be expressed as:

$$\rho^{ind}(\mathbf{r}, t) = -\nabla \cdot \mathbf{P}(\mathbf{r}, t) = -iq_{\parallel} en_e \Theta\left(z + \frac{L}{2}\right) \Theta\left(-z + \frac{L}{2}\right) \mathbf{\Delta}_0 e^{i\mathbf{q}_{\parallel} \cdot \mathbf{r} - i\omega t}$$

This density can be seen as a distribution of planes orthogonal to the z axis, each of them containing a surface distribution of charge oscillating in time and spatially modulated by a wave vector \mathbf{q}_{\parallel} . It can be rewritten as:

$$\rho^{ind}(\mathbf{r}, t) = -in_e eq_{\parallel} \mathbf{\Delta}_0 \int_{-L/2}^{L/2} dz' \delta(z - z') e^{iq_{\parallel} r_{\parallel} - i\omega t} \quad (\text{B1})$$

The potential induced by a planar distribution of charge of the form $e^{iq_{\parallel}r_{\parallel}}$ located in z' it is given by

$$v(\mathbf{q}_{\parallel}, z, z') = \frac{2\pi}{|\mathbf{q}_{\parallel}|} e^{-|\mathbf{q}_{\parallel}||z-z'|}$$

The potential induced by (B1) is:

$$\phi^{ind} = \int_{-L/2}^{L/2} dz' v(\mathbf{q}_{\parallel}, z, z') \rho^{ind}(\mathbf{r}', t) = -\frac{2\pi}{|\mathbf{q}_{\parallel}|} ien_e q_{\parallel} \Delta_0 e^{iq_{\parallel}r_{\parallel} - i\omega t} \int_{-L/2}^{L/2} dz' e^{-|\mathbf{q}_{\parallel}||z-z'|}$$

The integral must be evaluated for the three region of the space $z < -L/2$, $-L/2 < z < L/2$ and $z > L/2$. It comes:

$$\int_{-L/2}^{L/2} dz' e^{-|\mathbf{q}_{\parallel}||z-z'|} = \begin{cases} \frac{2}{|\mathbf{q}_{\parallel}|} e^{-|\mathbf{q}_{\parallel}|z} \sinh(|\mathbf{q}_{\parallel}|L/2) & \text{for } z > L/2 \\ \frac{1}{|\mathbf{q}_{\parallel}|} \left[2 - 2e^{-|\mathbf{q}_{\parallel}|\frac{L}{2}} \cosh(|\mathbf{q}_{\parallel}|z) \right] & \text{for } -L/2 < z < L/2 \\ \frac{2}{|\mathbf{q}_{\parallel}|} e^{|\mathbf{q}_{\parallel}|z} \sinh(|\mathbf{q}_{\parallel}|L/2) & \text{for } z < -L/2 \end{cases}$$

The induced potential is then:

$$\phi^{ind} = -\frac{4\pi}{|\mathbf{q}_{\parallel}|} ien_e q_{\parallel} F(z) \Delta_0 e^{iq_{\parallel}r_{\parallel} - i\omega t}$$

where we have defined, for sake of clarity, the function $F(z)$:

$$F(z) = \begin{cases} e^{-|\mathbf{q}_{\parallel}|z} \sinh(|\mathbf{q}_{\parallel}|L/2) & \text{for } z > L/2 \\ \left[1 - e^{-|\mathbf{q}_{\parallel}|\frac{L}{2}} \cosh(|\mathbf{q}_{\parallel}|z) \right] & \text{for } -L/2 < z < L/2 \\ e^{|\mathbf{q}_{\parallel}|z} \sinh(|\mathbf{q}_{\parallel}|L/2) & \text{for } z < -L/2 \end{cases}$$

Appendix C: Transverse polarization from longitudinal perturbation

In a thin slab, a longitudinal perturbation parallel to the surface can induce a polarization containing also a transverse part. When a vector field $\mathbf{V}(\mathbf{r}) = \mathbf{V}_0(\mathbf{r}) e^{i\mathbf{q}\cdot\mathbf{r}}$ has a spatial dependency which is not only contained in the plane-wave part $e^{i\mathbf{q}\cdot\mathbf{r}}$, the transverse or longitudinal nature is not simply related to the direction of the field compared to the wave vector \mathbf{q} . It must be seen for each Fourier component $\tilde{\mathbf{V}}(\mathbf{k})$, which is achieved by the calculation of the divergence or the curl of the field [50, 51].

$$\text{For a purely transverse field: } \nabla \cdot \mathbf{V}(\mathbf{r}) \equiv 0 \iff i\mathbf{k} \cdot \tilde{\mathbf{V}}(\mathbf{k}) \equiv 0 \quad \forall \mathbf{k}$$

$$\text{For a purely longitudinal field: } \nabla \times \mathbf{V}(\mathbf{r}) \equiv 0 \iff i\mathbf{k} \times \tilde{\mathbf{V}}(\mathbf{k}) \equiv 0 \quad \forall \mathbf{k}$$

For the induced field we have:

$$\nabla \times \mathbf{E}^{ind} = \nabla \times \nabla \phi^{ind} \equiv 0$$

For the polarization (Eq. (20)) we have:

$$\nabla \times \mathbf{P} = \begin{pmatrix} 0 \\ \partial_z P_x \\ 0 \end{pmatrix} = \begin{pmatrix} 0 \\ [\delta(z + \frac{L}{2}) - \delta(-z + \frac{L}{2})] en_e e^{iq_{\parallel}r_{\parallel} - i\omega t} \\ 0 \end{pmatrix} \neq 0 \quad (\text{C1})$$

This establishes that the induced polarization contains a transverse part, while the induced electric field is purely longitudinal.

- [1] M. Chhowalla, D. Jena, and H. Zhang, Two-dimensional semiconductors for transistors, *Nature Reviews Materials* **1**, 16052 (2016).
- [2] G. Iannaccone, F. Bonaccorso, L. Colombo, and G. Fiori, Quantum engineering of transistors based on 2d materials heterostructures, *Nature Nanotechnology* **13**, 183 (2018).
- [3] S. Ögüt, J. R. Chelikowsky, and S. G. Louie, Quantum confinement and optical gaps in si nanocrystals, *Phys. Rev. Lett.* **79**, 1770 (1997).
- [4] C. Delerue, G. Allan, and M. Lannoo, Dimensionality-dependent self-energy corrections and exchange-correlation potential in semiconductor nanostructures, *Phys. Rev. Lett.* **90**, 076803 (2003).
- [5] L. Wirtz, A. Marini, and A. Rubio, Excitons in boron nitride nanotubes: Dimensionality effects, *Phys. Rev. Lett.* **96**, 126104 (2006).
- [6] K. F. Mak, C. Lee, J. Hone, J. Shan, and T. F. Heinz, Atomically thin mos₂: A new direct-gap semiconductor, *Phys. Rev. Lett.* **105**, 136805 (2010).
- [7] G. Onida, L. Reining, and A. Rubio, Electronic excitations: density-functional versus many-body green's-function approaches, *Rev. Mod. Phys.* **74**, 601 (2002).
- [8] E. Runge and E. K. U. Gross, Density-functional theory for time-dependent systems, *Phys. Rev. Lett.* **52**, 997 (1984).
- [9] E. K. U. Gross and W. Kohn, Local density-functional theory of frequency-dependent linear response, *Phys. Rev. Lett.* **55**, 2850 (1985).
- [10] R. van Leeuwen, Mapping from densities to potentials in time-dependent density-functional theory, *Phys. Rev. Lett.* **82**, 3863 (1999).
- [11] C. Ullrich, *Time-Dependent Density-Functional Theory: Concepts and Applications*, Oxford Graduate Texts (OUP Oxford, 2012).
- [12] L. Reining, V. Olevano, A. Rubio, and G. Onida, Excitonic effects in solids described by time-dependent density-functional theory, *Phys. Rev. Lett.* **88**, 066404 (2002).
- [13] S. L. Adler, Quantum theory of the dielectric constant in real solids, *Phys. Rev.* **126**, 413 (1962).
- [14] N. Wiser, Dielectric constant with local field effects included, *Phys. Rev.* **129**, 62 (1963).
- [15] H. Ehrenreich, Electromagnetic transport in solids: optical properties and plasma effects, in *The Optical Properties of Solids*, edited by J. Tauc (1966) p. 106.
- [16] C. A. Rozzi, D. Varsano, A. Marini, E. K. U. Gross, and A. Rubio, Exact coulomb cutoff technique for supercell calculations, *Phys. Rev. B* **73**, 205119 (2006).
- [17] S. Ismail-Beigi, Truncation of periodic image interactions for confined systems, *Phys. Rev. B* **73**, 233103 (2006).
- [18] N. Tancogne-Dejean, C. Giorgetti, and V. Véniard, Optical properties of surfaces with supercell ab initio calculations: Local-field effects, *Phys. Rev. B* **92**, 245308 (2015).
- [19] K. S. Novoselov, A. K. Geim, S. V. Morozov, D. Jiang, Y. Zhang, S. V. Dubonos, I. V. Grigorieva, and A. A. Firsov, Electric field effect in atomically thin carbon films, *Science* **306**, 666 (2004), <https://www.science.org/doi/pdf/10.1126/science.1102896>.
- [20] F. Hüser, T. Olsen, and K. S. Thygesen, How dielectric screening in two-dimensional crystals affects the convergence of excited-state calculations: Monolayer mos₂, *Phys. Rev. B* **88**, 245309 (2013).
- [21] F. A. Rasmussen, P. S. Schmidt, K. T. Winther, and K. S. Thygesen, Efficient many-body calculations for two-dimensional materials using exact limits for the screened potential: Band gaps of mos₂, h-bn, and phosphorene, *Phys. Rev. B* **94**, 155406 (2016).
- [22] K. S. Thygesen, Calculating excitons, plasmons, and quasiparticles in 2d materials and van der waals heterostructures, *2D materials* **4**, 022004 (2017).
- [23] Y. Li, A. Chernikov, X. Zhang, A. Rigosi, H. M. Hill, A. M. van der Zande, D. A. Chenet, E.-M. Shih, J. Hone, and T. F. Heinz, Measurement of the optical dielectric function of monolayer transition-metal dichalcogenides: MoS₂, MoSe₂, WS₂, and WSe₂, *Phys. Rev. B* **90**, 205422 (2014).
- [24] S. Funke, B. Miller, E. Parzinger, P. Thiesen, A. W. Holleitner, and U. Wurstbauer, Imaging spectroscopic ellipsometry of MoS₂, *Journal of Physics: Condensed Matter* **28**, 385301 (2016).
- [25] Yambo, Yambo forum, http://www.yambo-code.org/wiki/index.php?title=How_to_treat_low_dimensional_systems.
- [26] A. Molina-Sánchez, G. Catarina, D. Sangalli, and J. Fernández-Rossier, Magneto-optical response of chromium trihalide monolayers: chemical trends, *Journal of Materials Chemistry C* **8**, 8856–8863 (2020).
- [27] P. Cudazzo, I. V. Tokatly, and A. Rubio, Dielectric screening in two-dimensional insulators: Implications for excitonic and impurity states in graphane, *Phys. Rev. B* **84**, 085406 (2011).
- [28] A. Laturia, M. L. Van de Put, and W. G. Vandenberghe, Dielectric properties of hexagonal boron nitride and transition metal dichalcogenides: from monolayer to bulk, *npj 2D Materials and Applications* **2**, 6 (2018).
- [29] D. E. Aspnes, Optical properties of thin films, *Thin solid films* **89**, 249 (1982).
- [30] T. Tian, D. Scullion, D. Hughes, L. H. Li, C.-J. Shih, J. Coleman, M. Chhowalla, and E. J. G. Santos, Electronic polarizability as the fundamental variable in the dielectric properties of two-dimensional materials, *Nano Letters* **20**, 841 (2020), pMID: 31888332, <https://doi.org/10.1021/acs.nanolett.9b02982>.
- [31] M. Royo and M. Stengel, Exact long-range dielectric screening and interatomic force constants in quasi-two-dimensional crystals, *Phys. Rev. X* **11**, 041027 (2021).
- [32] M. Palummo, G. Onida, R. Del Sole, and B. S. Mendoza, Ab initio optical properties of si(100), *Phys. Rev. B* **60**, 2522 (1999).
- [33] P. Hohenberg and W. Kohn, Inhomogeneous electron gas, *Phys. Rev.* **136**, B864 (1964).
- [34] W. Kohn and L. J. Sham, Self-consistent equations including exchange and correlation effects, *Phys. Rev.* **140**, A1133 (1965).
- [35] X. Gonze, F. Jollet, F. A. Araujo, D. Adams, B. Amadon, T. Applencourt, C. Audouze, J.-M. Beuken, J. Bieder, A. Bokhanchuk, E. Bousquet, F. Bruneval, D. Caliste, M. Côté, F. Dahm, F. D. Pieve, M. Delaveau, M. D. Genaro, B. Dorado, C. Espejo, G. Geneste, L. Genovese, A. Gerossier, M. Giantomassi, Y. Gillet, D. Hamann, L. He, G. Jomard, J. L. Janssen, S. L. Roux, A. Levitt,

- A. Lherbier, F. Liu, I. Lukacevic, A. Martin, C. Martins, M. Oliveira, S. Poncé, Y. Pouillon, T. Rangel, G.-M. Rignanese, A. Romero, B. Rousseau, O. Rubel, A. Shukri, M. Stankovski, M. Torrent, M. V. Setten, B. V. Troeye, M. Verstraete, D. Waroquier, J. Wiktor, B. Xue, A. Zhou, and J. Zwanziger, Recent developments in the ABINIT software package, *Computer Physics Communications* **205**, 106 (2016).
- [36] Francesco Sottile, Lucia Reining and Valerio Olevano, The dp code, https://etsf.polytechnique.fr/software/Ab_Initio/.
- [37] N. Tancogne-Dejean, *Ab initio description of second-harmonic generation from crystal surfaces*, Theses, Ecole polytechnique (2015), <https://pastel.archives-ouvertes.fr/tel-01235611>.
- [38] V. M. Silkin, E. V. Chulkov, and P. M. Echenique, Band structure versus dynamical exchange-correlation effects in surface plasmon energy and damping: A first-principles calculation, *Phys. Rev. Lett.* **93**, 176801 (2004).
- [39] V. Kenner, R. Allen, and W. Saslow, Screening of external fields and distribution of excess charge near a metal surface, *Physics Letters A* **38**, 255 (1972).
- [40] N. D. Lang and W. Kohn, Theory of metal surfaces: Charge density and surface energy, *Phys. Rev. B* **1**, 4555 (1970).
- [41] E. K. Yu, D. A. Stewart, and S. Tiwari, Ab initio study of polarizability and induced charge densities in multilayer graphene films, *Phys. Rev. B* **77**, 195406 (2008).
- [42] Y. Yang, K. Zhong, G. Xu, J.-M. Zhang, and Z. Huang, Electronic structure and its external electric field modulation of pbpd2 ultrathin slabs with (002) and (211) preferred orientations, *Scientific Reports* **7**, 6898 (2017).
- [43] R. Del Sole and E. Fiorino, Macroscopic dielectric tensor at crystal surfaces, *Phys. Rev. B* **29**, 4631 (1984).
- [44] M. Schubert, Polarization-dependent optical parameters of arbitrarily anisotropic homogeneous layered systems, *Phys. Rev. B* **53**, 4265 (1996).
- [45] G. B. Airy M.A. F.R.A.S. F.G.S., Vi. on the phenomena of newton's rings when formed between two transparent substances of different refractive powers, *The London, Edinburgh, and Dublin Philosophical Magazine and Journal of Science* **2**, 20 (1833), <https://doi.org/10.1080/14786443308647959>.
- [46] Abeles, Florin, Recherches sur la propagation des ondes électromagnétiques sinusoïdales dans les milieux stratifiés - application aux couches minces, *Ann. Phys.* **12**, 596 (1950).
- [47] M. Born and E. Wolf, *Principles of Optics* (Cambridge University Press, 2019).
- [48] P. Yeh, *Optical Waves in Layered Media*, Wiley Series in Pure and Applied Optics (Wiley, 2005).
- [49] G. Grosso and G. Parravicini, *Solid State Physics* (Elsevier Science, 2000).
- [50] C. Cohen-Tannoudji, J. Dupont-Roc, and G. Grynberg, *Photons et atomes. Introduction à l'électrodynamique quantique: Introduction à l'électrodynamique quantique*, SAVOIRS ACTUELS (EDP Sciences, 2012).
- [51] H. Helmholtz, Lxiii. on integrals of the hydrodynamical equations, which express vortex-motion, *The London, Edinburgh, and Dublin Philosophical Magazine and Journal of Science* **33**, 485 (1867), <https://doi.org/10.1080/14786446708639824>.